Available online at www.sciencedirect.com
SCIENCE DIRECT®
ELSEVIER
Coordination Chemistry Reviews 248 (2004) 279–297
COORDINATION CHEMISTRY REVIEWS
www.elsevier.com/locate/ccr

Review

From long-chain conjugated oligomers to dendrimers: synthesis and physical properties of phenyl-ethenyl-ferrocenyl containing one- and two-dimensional complexes

Eduardo Peris*

Dpto. de Química Inorgánica y Orgánica, Universitat Jaume I, 12071 Castellón, Spain

Received 12 September 2003; accepted 19 January 2004

Contents

Abstract

This review article presents an overview of the chemistry of phenyl-ethenyl oligomers containing ferrocene. The synthetic procedures, electronic spectra, electrochemistry and molecular structures are briefly described, pursuing a rationalized relation with the physical outputs (especially regarding the nonlinear optical responses). All the properties of the compounds described are clearly dependent on the conjugated character of the ancillary ligands of the ferrocene. Three types of complexes are described: mono-dimensional conjugated oligomers, compounds with linked ferrocenes, and two-dimensional star-shaped (dendrimers) ferrocenyl compounds.

Keywords: Phenyl-ethenyl oligomers; One- and two-dimensional complexes; Ferrocene

1. Introduction

During the last three decades, much attention has been devoted to the chemistry of ferrocenyl complexes because ferrocene combines chemical versatility with high

---

* Fax: +34-964-728214.
E-mail address: eperis@qio.uji.es (E. Peris).

0010-8545/$ – see front matter © 2004 Elsevier B.V. All rights reserved.
doi:10.1016/j.ccr.2004.01.006

thermal stability. These properties, together with the exceptional electrochemical properties of ferrocene, make ferrocene-based complexes good candidates for the preparation of new materials with applications in organic synthesis, catalysis and materials science [1,2]. When two or more ferrocenyl fragments are connected to obtain compounds with linked ferrocenes, further interests are envisaged, since intermetallic electronic communication affords a wide range of new applications, and many studies have been made regarding intramolecular electron-exchange reactions [3–6].

Metal containing long-chain conjugated systems have emerged as an important category of materials. The impetus for developing these materials is based on the premise that conjugated chains containing metals are expected to possess properties significantly different from those of conventional organic conjugated oligomers. Examples of these properties include: electrical conductivity, magnetic behavior, thermal stability, nonlinear optical (NLO) effects, and even superconductivity. Because of the special electronic and chemical properties of ferrocene, many efforts have been directed towards the incorporation of a ferrocene moiety into a polymer [1,2] in order to investigate novel properties such as those mentioned above. Although there have been many studies reported where metallocene-containing long-chained conjugated systems are obtained [3,6–9], there still lacks systematic descriptions of syntheses leading to useful starting materials. In fact, the bottleneck to the development of organometallic push–pull oligomers is the lack of systematic approaches to the synthesis of long-chained conjugated systems. All the metal-containing polymers which have been reported, have in common that they are only conducting if charge carriers can be delocalized over both the metal and the organic fragments. In this regard, we have focused our attention on the fabrication, characterization and study of several types of ferrocene-containing conjugated oligomers, paying special attention to the relation between their chemical structures and their physical outputs.

In this paper, several phenyl-ethenyl ferrocenyl containing oligomers are described, specially with (i) pendant electron-accepting groups (nitro, pyridine, nitrile and heterometallic complexes derived from the coordination of the two latter terminations), (ii) linked ferrocenes, and (iii) two-dimensional star-shaped structures (or metallodendrimers).

2. One-dimensional ferrocenyl-phenyl-ethenyl oligomers

The idea of end-capping a phenyl-ethenyl oligomer with a ferrocenyl fragment, comes from the wide range of options that this system can offer to the design of metal-containing oligomers. Ferrocene has been widely considered as a moderate electron-donating fragment [1,2,10], so the connection to an electron-accepting moiety through a conjugated chain may afford the preparation of push–pull oligomers with interesting physical properties (Scheme 1). Among the applications that we pursued for our oligomers, we were specially interested in those derived from the NLO responses, and in clarifying if there were any clear relationships between the chemical structures, physical properties (electronic spectra, electrochemistry) and NLO behavior of the complexes obtained.

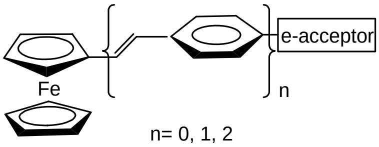

Scheme 1.

2.1. Synthesis of the compounds

Most of the ferrocenyl-based conjugated oligomers reported to date, have been obtained by conventional Wittig–Horner (WH) reactions, but these reactions usually lead to the formation of *E* and *Z* isomer mixtures [11–14]. Several authors have reported the advantages of the *E*-type isomers over the *Z*-type for effective electronic coupling [15,16]. The lack of coplanarity between donor and acceptor groups in the *Z* isomers leads to a decrease in their electronic communication. In addition, the reduction of the through space distance (in the *Z*-type) between donor and acceptor results in a lower change in dipole per unit charge separation. Since most of the times the aim of the synthetic procedures is to obtain linear oligomers with effective electronic coupling, the *E* isomers are the ones that are mainly pursued, but the separation of the mixtures of the *E* and *Z* isomers is not always easy. In our first study, we reported the preparation and characterization of simple ferrocenyl-based ligands with end capped nitrile, pyridyl and phenyl groups [17]. The synthetic process was based in the olefination of aldehydes by the Wittig method, yielding mixtures of *Z* and *E* isomers which could be conveniently separated (Scheme 2). The end-capping groups allowed the preparation of heterometallic σ-bound (CN and pyr cases) and π-bound (phenyl) complexes, by reacting these ligands with $M(CO)_6$ (M = Cr, Mo, W).

When we used the same reaction (WH) in order to obtain the longer chained compounds, we unexpectedly observed that the only characterizable spectroscopically and isolable compounds were the (*E*,*Z*) and (*E*,*E*,*Z*) isomers (the first number always corresponds to the double bond nearest to the ferrocenyl group). For reasons that we still do not know, stereolinear isomers (*E*,*E*) and (*E*,*E*,*E*) were not obtained by this procedure. In order to obtain these isomers we performed the corresponding Horner–Emmons–Wadsworth (HEW) reaction that stereoselectively lead to the formation of double bonds in the *E*-configuration [18]. As it is shown in Scheme 3, (*E*,*E*) and (*E*,*E*,*E*) compounds were obtained by double olefination of *p*-xylenebis(diethylphosphonate) with the ferrocenyl-aldehyde compound (*E*)-CHO or (*E*,*E*)-CHO

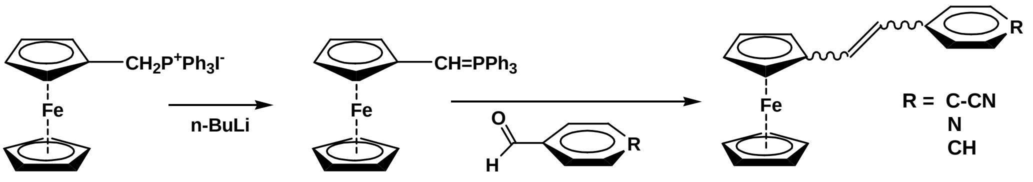

Scheme 2.

and the corresponding 4-substituted-benzaldehyde. This procedure leads to reasonably good yields for compounds (*E*,*E*), but compounds (*E*,*E*,*E*) are only obtained in extremely low yield. We tried to obtain the *E*-isomers by isomerization of the *Z* isomers using *N*-bromosuccinimide and I_2 or with basic alumina, but no conversion was observed.

Another problem that we found in the preparation of these ferrocenyl complexes, came from the synthetic routes to the carboxaldehyde intermediates (*E*)-CHO and (*E*,*E*)-CHO. The synthetic routes for such complexes lead, in most cases, to moderate to poor yields [11], and the separation workups make the overall process complicated. In

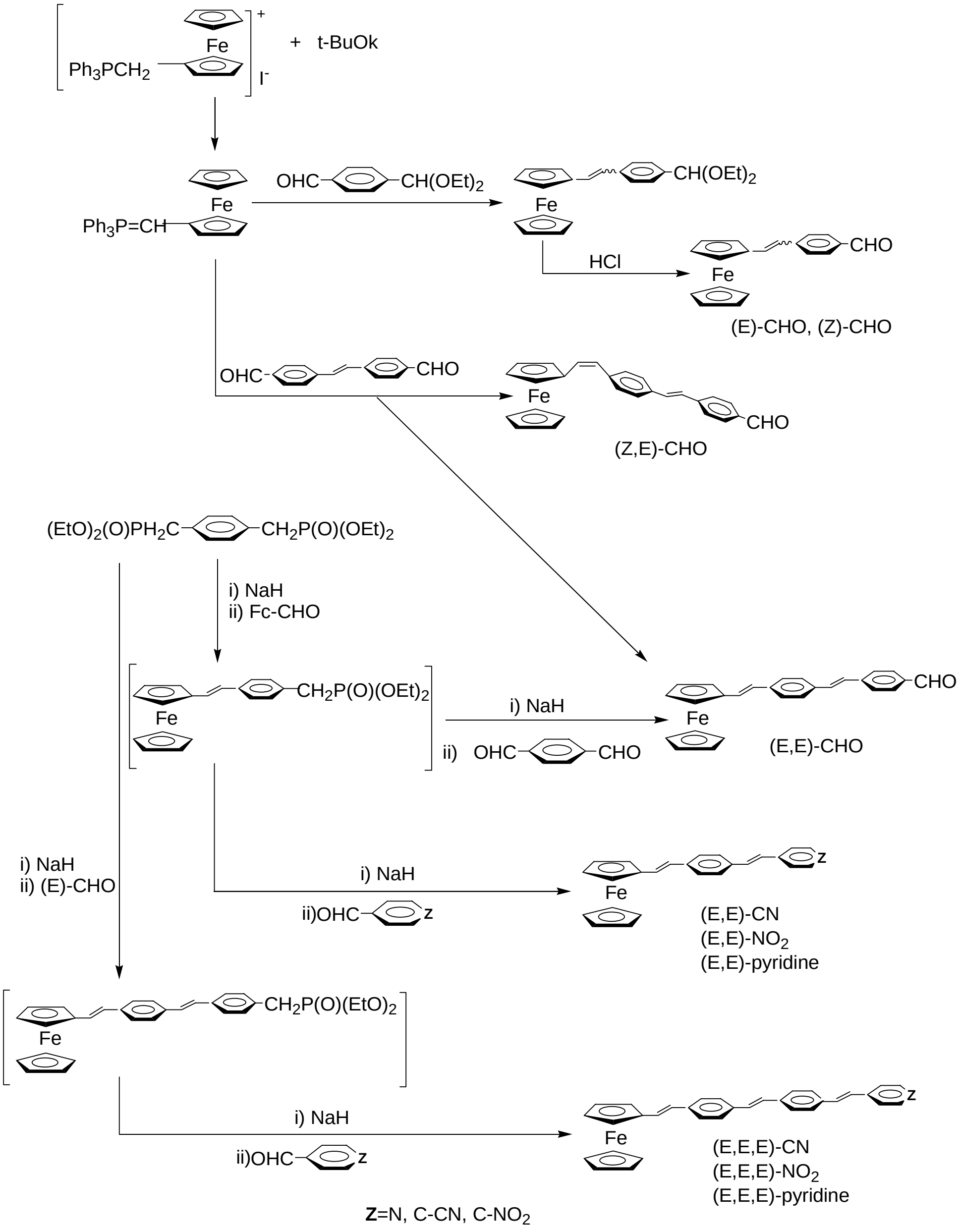

Scheme 3.

order to simplify the preparation of these intermediates, we modified their synthesis as it is shown in Scheme 3. The use of terephthalaldehydemono-(diethylacetal) [p-OHC-C_6H_4-CH(OEt)$_2$] instead of the more widely used terephthaldehyde (p-OHC-C_6H_4-CHO), avoids the formation of 1,4-bis(ferrocenyl)ethenylbenzene as one of the major side-products of these types of reactions. The ferrocenyl-acetal complex so synthesized, can be transformed into the carboxaldehyde compound, by simply reacting the acetal derivative in a solution of hydrochloric acid as has already been reported [14].

The use of *p*-xylenebis(diethylphosphonate) in the HEW reactions leads to the formation of *E* isomers in relatively good yield for the cases where the number of phenyl-ethenyl units is 1 and 2, but it did not lead to favorable results for synthesis of longer oligomers. This is a general fact that affects all the compounds obtained with end-capping nitrile, pyridine and nitro. We believe that this unfavourable result may be due to the extremely low solubility of the compounds containing more than three phenyl-ethenyl units, which would be formed by this method. This low solubility, probably due to the rigid-row geometry derived from the all-*E* configuration, complicates the characterization of these complexes (if formed) by conventional methods and, furthermore, would explain the loss of the aforementioned compounds during the extraction of compounds made in the last step of the olefination.

Pyridine and nitrile terminated ferrocenyl compounds can be coordinated to metal carbonyl fragments $M(CO)_5$ (M = Cr, Mo, W) giving heterobimetallic push–pull complexes. Scheme 4 shows the general synthetic route.

2.2. Electronic spectra

The current interest in the use of organic and organometallic materials in second nonlinear optics prompted us to determine the suitability of these ferrocenyl derivatives by carefully studying their electronic spectra. Solvatochromic effects can hint to the magnitude of the expected NLO properties, since they reflect the polarizability of a chromophore [11,19]. In general, the electronic absorption spectra of the ferrocenyl mono-substituted compounds show one prominent band between 300 nm and 390 nm assigned to π–π^* transitions, according to the data in the literature [9,12,14,15,17,20–22]. Another weaker band at higher wavelengths (about 500 nm), is attributed to a metal-to-ligand charge-transfer (MLCT) band, and d–d transitions are only discernible in some cases as a shoulder on the MLCT band. This assignment is in accordance with the theoretical results reported by Barlow et al. (model III in Ref. [9]) and to other experimental results [9,12,14,15,17,20–22] although we are aware that there is some controversy about this assignment [23]. In the compounds that we report here, only one band for the π–π^* transitions is clearly observed being strongly influenced by the length of the conjugated ancillary ligand. The band is redshifted with increasing polyenic length only in the cases in which the addition of the phenylene-vinylene unit is produced in the *E* form. This effect can be clearly seen in Fig. 1 for the case of two ferrocenyl–nitro compounds with different chain lengths. The same effect is observed for the compounds terminated with nitrile and pyridine fragments, as can be seen in Table 1. This result indicates that elongation of the conjugation length lowers the energy of the π^* orbital only if the elongation is produced in the *E* form. On going from the *E* to the *Z* isomers, we observe that there is a bathochromic shift of the π–π^* transition indicating that the π^* orbital is less stabilized than in the case of the *E* isomers. This effect is due to a partially loss of the conjugation as a consequence of the non-coplanar geometry imposed by the configuration of the complex. The lower energy band (MLCT) also shows a clear dependence on the chain length of the polyenic ligand, but the effect is of a lower magnitude than for the higher energy band (π–π^*). As a result, the two bands overlap for long ferrocene oligomers avoiding a clear assignment of a frequency to the MLCT transitions.

A redshift is also observed in the cases in which an electron-accepting moiety is coordinated to the ligand (see the $Cr(CO)_5$ and $W(CO)_5$ cases in Table 1), these changes being much more appreciable for the (*E*,*E*) isomers, according to their greater charge transfer capabilities.

We believe that an interesting point can be drawn from a comparison of the electronic spectroscopic data for the methylated ferrocenyl–pyridine complexes (Table 1). A nonlinear increase in the value of λ ($\pi-\pi^*$) is observed upon chain-lengthening, suggesting different net contributions for each phenylene-vinylene subunit. These data (although limited to only three points) suggest that an effective limit for

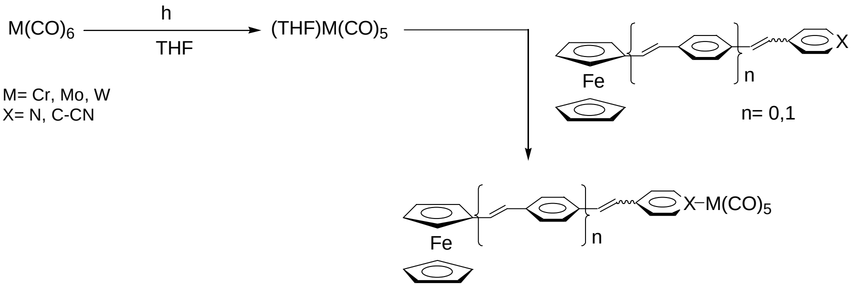

Scheme 4.

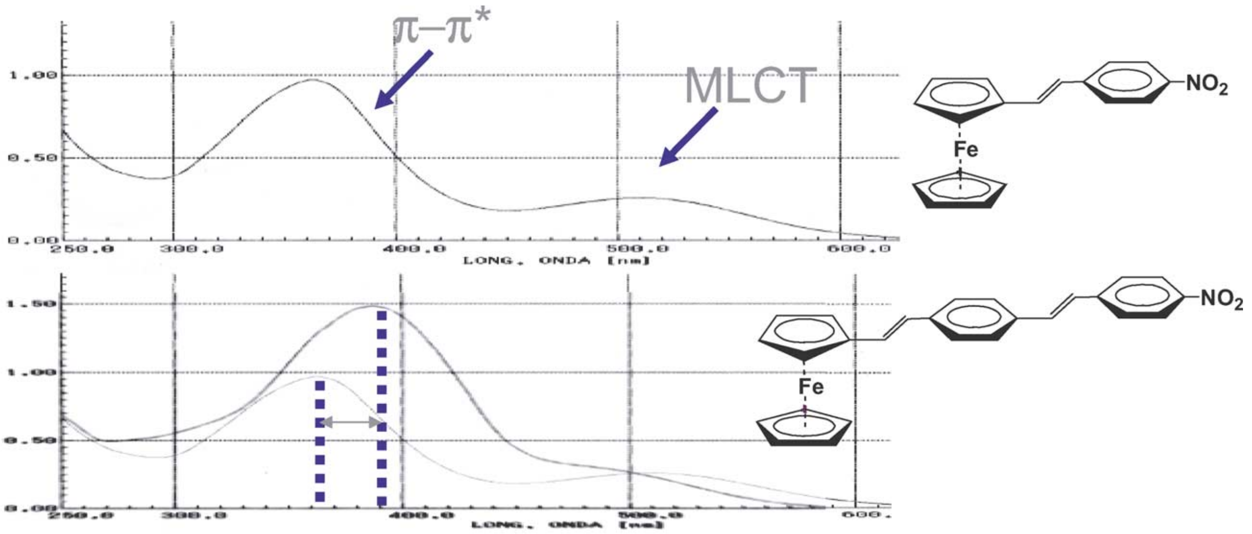

Fig. 1. UV-Vis spectra of compounds {(*E*)-(η^5-C_5H_5)Fe(η^5-C_5H_4)[(CH=CH)(C_6H_4)]NO_2}, (*E*)-NO_2, and {(*E*,*E*)-(η^5-C_5H_5)Fe(η^5-C_5H_4)[(CH=CH)(C_6H_4)]$_2$$NO_2$}, (*E*,*E*)-$NO_2$, showing the redshift of the π–π* band upon elongating the conjugated chain.

Table 1
Electronic spectra data for several representative ferrocenyl–nitro, –pyridine and –nitrile complexes (in $CHCl_3$)

Compound	λ/π–π* (nm)	Compound	λ/π–π* (nm)
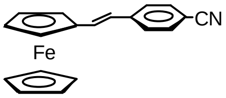	329	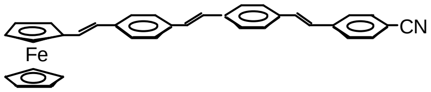	380
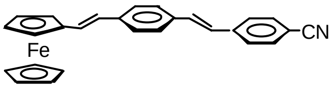	340	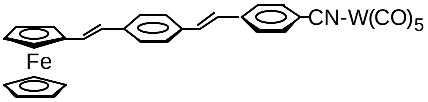	394
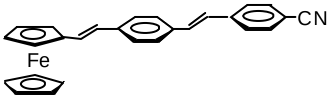	369	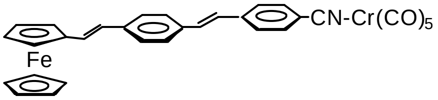	380
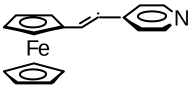	315	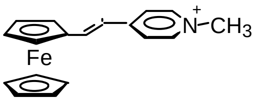	361
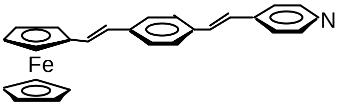	358	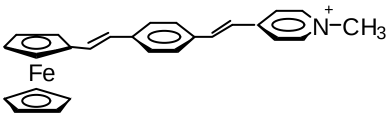	402
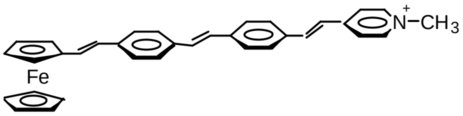	417	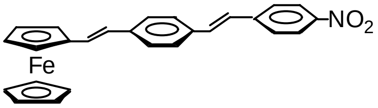	388
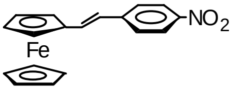	363		

conjugation may be envisaged, this being supported by the results reported by Hsung et al. [24] where again, a nonlinear shift of λ_{max} is observed upon elongating the chain of a series of ferrocenyl-based phenylethynyl oligomers.

In the literature, we have found that smaller shifts in λ are observed upon changing the solvent for the high-energy band (π–π^*) [9] whilst larger solvatochromic shifts are observed for the low energy bands. The same effect is seen for our ferrocenyl-based compounds. A small and negative solvatochromic effect is observed for the π–π^* transition band (higher energy band) in all the compounds that we studied. This effect is also observed for the lower energy band (MLCT), this being more solvatochromic than the higher energy one (π–π^*).

2.3. Electrochemistry

Electrochemistry offers the possibility to examine trends in LUMO energies. The electrochemical data obtained for some of the most representative compounds in this study are summarized in Table 2. All the compounds were measured in CH_2Cl_2 using the same setup. In all cases, we observed the chemically reversible ferrocenium/ferrocene couple with $i_{pa}/i_{pc} \cong 1$. Although the peak to peak separations in all compounds were greater than the ideal value for a fully reversible one-electron process, this difference ($E_{pc} - E_{pa}$) is similar to that measured for ferrocene under the conditions of the experiment. Addition of the electron-accepting fragment to ferrocene, results in a increase of the redox potential compared to that of unsubstituted ferrocene (445 mV). This effect has been studied in detail by Barlow et al. [9] Chain lengthening promotes a decrease in the redox potential, probably due to the stabilization of the positive charge of the oxidized species along the conjugated chain. This effect is especially seen in the *E*-type complexes, where the stabilization of the positive charge along the conjugated chain is better achieved as observed by the larger decrease of the redox potential than that observed for the *Z*-type oligomers.

For the cationic methylated ferrocenyl-pyridiniumyl compounds, there is a large cathodic shift when going from [(*E*)-(η^5-C_5H_5)Fe(η^5-C_5H_4)(CH=CH)(C_5H_4N-CH_3)]$^+$, (*E*)-*N*-CH_3, to [(*E*,*E*)-(η^5-C_5H_5)Fe(η^5-C_5H_4)[(CH=CH)(C_6H_4)]-

Table 2
Cyclic voltammetric data for some representative ferrocenyl–nitro, –pyridine and –nitrile complexes

Compound	$E_{1/2}$ (ΔE_p)	Compound	$E_{1/2}$ (ΔE_p)
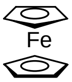	446 (106)	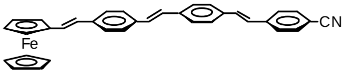	420 (85)
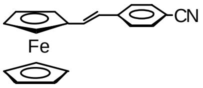	480 (80)	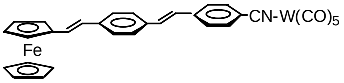	435 (80)
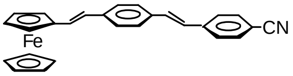	445 (70)	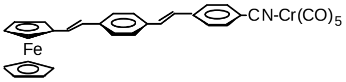	435 (85)
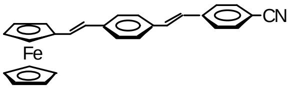	440 (70)	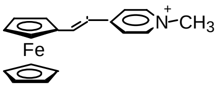	596 (84)[a]
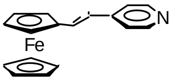	468 (70)	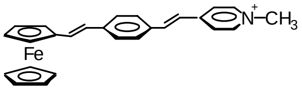	384 (78)[a]
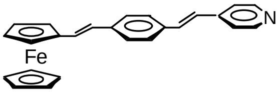	440 (67)	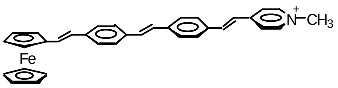	357 (67)[a]
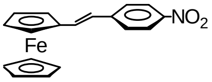	500 (100)	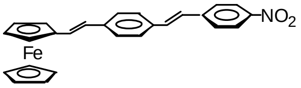	445 (100)
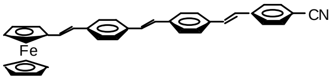	428 (70)		

$E_{1/2}$ and ΔE_p in millivolt. Measured in $CHCl_3$.

[a] Measured in acetone.

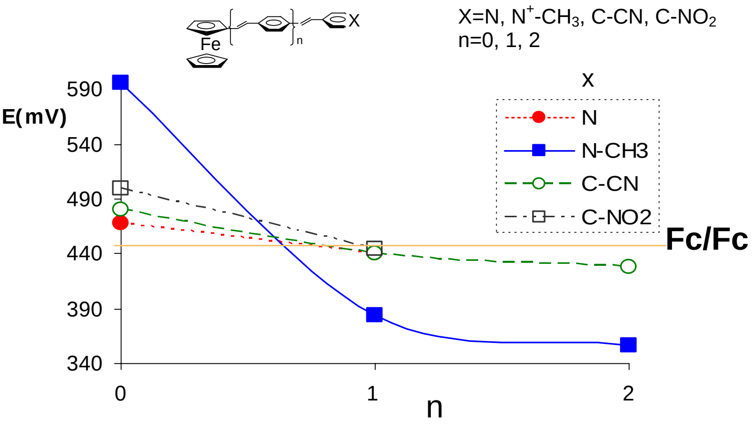

Fig. 2. Redox potentials (ferrocene-based, *E* (mV)) vs. number of vinyl-phenylene subunits (*n*).

$(CH{=}CH)(C_5H_4N\text{-}CH_3)]^+$, (*E*,*E*)-*N*-$CH_3$, but much less important when adding a new vinyl-phenylene subunit to obtain $[(E,E,E)\text{-}(\eta^5\text{-}C_5H_5)Fe(\eta^5\text{-}C_5H_4)[(CH{=}CH)(C_6H_4)]_2(CH{=}CH)(C_5H_4N\text{-}CH_3)]^+$, (*E*,*E*,*E*)-*N*-$CH_3$. A similar effect (although with a lower redox change between the compound with one and two vinyl-phenylene subunits) is observed for the ferrocenyl–nitrile complexes, for which addition of each vinyl-phenylene subunit also results in a nonlinear decrease of the redox potential. This effect can be observed when we plot the redox potentials (ferrocene-based) versus the number of conjugated double bonds (Fig. 2).

Humphrey and coworkers have reported that stepwise elongation of the conjugated chain in ruthenium acetylides, leads to an increase in the NLO responses of the material, but this increase is gradually less until an asymptotic or limit situation is achieved in which elongation of the chain does not lead to any further increase in the NLO responses [25]. This observation, together with our results, suggest that conjugation may reach a limiting effective length.

2.4. Molecular structures

Electronic communication between the terminal groups in a conjugated polymer is one objective to achieve in order to obtain interesting physical properties such as electrical conductivity, magnetic behavior, thermal stability, NLO effects, and even superconductivity. As we have seen in the two previous sections, electronic spectra and cyclic voltammetry can give us a good account of how the electronic properties of our complexes can be modified by the effect of chain-elongation. In a series of vinyl-phenylene complexes such as ours, coplanarity is playing an important role in the electronic communication along the complex, since it favors π-overlapping of the p_z orbitals of the oligomer facilitating conjugation to be more effective.

The study of the molecular structures of a series of ferrocenyl–vinyl-phenylene–pyridine complexes offered us an excellent opportunity to study how coplanarity changes upon elongating the oligomer chain. We were lucky that the pyridine complexes were easy to crystallize and afforded good single crystals suitable for X-ray diffraction [21].

In general, the two cyclopentadienyl (Cp) rings are slightly tilted (2.4–6.5°) with respect to each other. The iron distances to the substituted and unsubstituted rings and the C–C distances within these rings lie in the expected range. Except for compound (*E*,*Z*)-pyridine, with a *Z* olefinic geometry, the phenylene and pyridyl rings are roughly coplanar with the substituted Cp ring. The phenylene ring deviates from coplanarity with respect to the substituted Cp ring in 1.93 and 11.96° for compounds (*E*,*E*)-pyridine, and the methylated analogous (*E*,*E*)-*N*-CH_3, respectively. In addition, methylation of the pyridyl fragment promotes an increase in coplanarity of the pyridyl group with respect to the substituted Cp from 7.53° for (*E*,*E*)-pyridine to 1.91° for (*E*,*E*)-*N*-CH_3. In compound (*E*,*E*)-pyridine, the through space Fe–N distance, equals 14.8 Å, and the sum of the bond lengths corresponding to the conjugation pathway from Fe to N is 18.9 Å (Fig. 3). Almost the same through space distance between the Fe and N atoms is observed for the methylated compound (*E*,*E*)-*N*-CH_3 (14.4 Å), indicating that no significant modification of the conjugated backbone has occurred upon the methylation. Fig. 3 shows

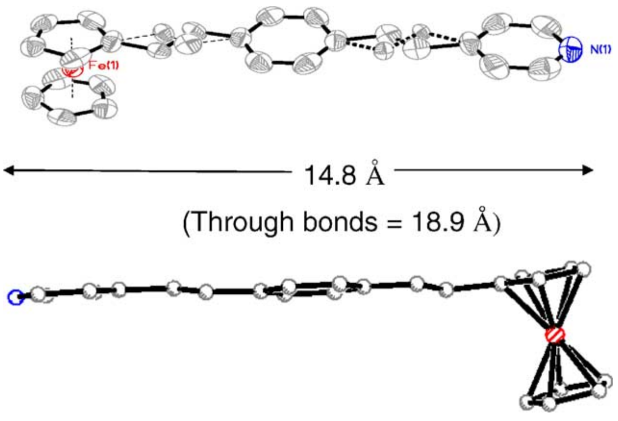

Fig. 3. Two perspectives of the molecular structure of $[(E,E)\text{-}(\eta^5\text{-}C_5H_5)Fe(\eta^5\text{-}C_5H_4)(CH{=}CH)(C_6H_4)(CH{=}CH)(C_5H_4N)]$, (*E*,*E*)-pyridine.

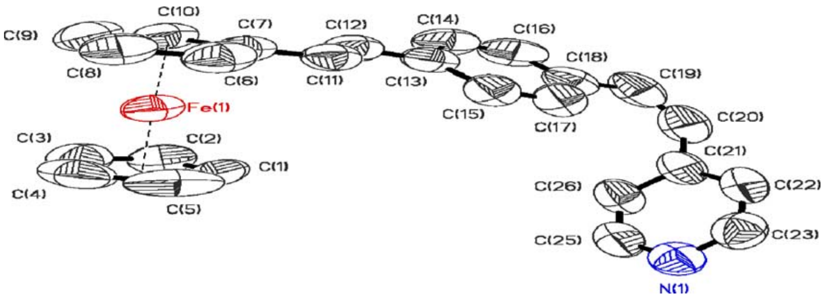

Fig. 4. Molecular structure of [(*E*,*Z*)-(η^5-C_5H_5)Fe(η^5-C_5H_4)[(CH=CH)(C_6H_4)(CH=CH)(C_5H_4N)], (*E*,*Z*)-pyridine.

two perspectives of the molecular structure of compound (*E*,*E*)-pyridine, in which clear coplanarity between the Cp and the pyridyl ring is observed.

As seen in Fig. 4, compound (*E*,*Z*)-pyridine, shows a large deviation from coplanarity with respect to the substituted Cp ring for both the phenylene and pyridyl rings as a consequence of the *Z* olefinic geometry. The linear arrangement is completely lost as seen from the Fe–N through space distance of 9.74 Å (compared with the 14.81 Å in (*E*,*E*)-pyridine).

The pyridinium compound (*E*,*E*,*E*)-*N*-CH_3 shows a Fe–N distance of 21.03 Å (through space) and 27.13 Å (through conjugated bonds). A clear loss of coplanarity with respect to the substituted Cp ring is observed, as seen by the interplanar angles of 8.73, 29.66, and 18.87° (from the first phenylene ring to the pyridyl fragment, respectively). The Cp to Cp (subs) interplanar angle is 6.49°, the highest of those of the compounds that we report, although this result may be mainly due to crystal packing effects (see Fig. 5).

Both ferrocenyl–pyridinium complexes, (*E*,*E*)-*N*-CH_3 and (*E*,*E*,*E*)-*N*-CH_3 show an eclipsed disposition of the Cp rings of the ferrocenyl fragment (Fig. 5), in contrast to the staggered disposition in the pyridyl complexes (*E*,*E*)-pyridine and (*E*,*Z*)-pyridine. This effect has already been described for other systems, and it has been pointed out that the electronic perturbation induced by oxidation of the iron atom or, in our case, the effective electronic communication from the positively charged pyridiniumyl moiety and the ferrocenyl fragment, may promote this change in the relative conformation of the two Cp rings in order to relieve steric strain induced by electronic perturbation [1].

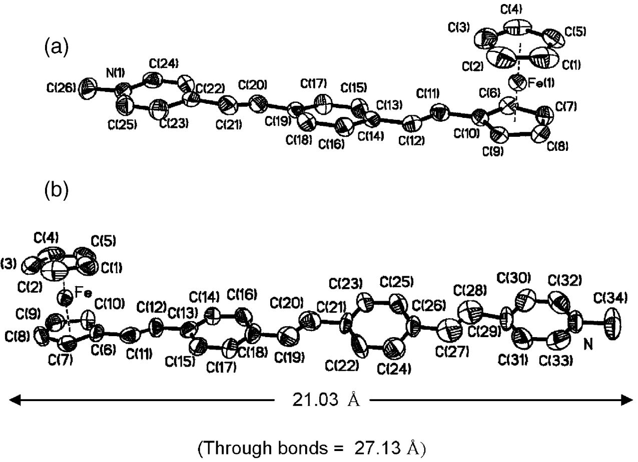

Fig. 5. Molecular structures of (a) [(*E*,*E*)-(η^5-C_5H_5)Fe(η^5-C_5H_4)[(CH=CH)(C_6H_4)](CH=CH)(C_5H_4N-CH_3)]$^+$, (*E*,*E*)-*N*-CH_3, and (b) [(*E*,*E*,*E*)-(η^5-C_5H_5)Fe(η^5-C_5H_4)[(CH=CH)(C_6H_4)]$_2$(CH=CH)(C_5H_4N-CH_3)]$^+$, (*E*,*E*,*E*)-*N*-CH_3.

In many cases, crystal packing determines the bulk physical properties of the compounds. In particular, if we are pursuing high bulk NLO responses, we will have to take into account that crystallization in a centrosymmeteric space group ensures canceling of the dipolar nature of the molecule and hence annuls the second order nonlinear responses. In this sense, the ferrocenyl–nitro complex, (*E*)-(η^5-C_5H_5)Fe(η^5-C_5H_4)(CH=CH)(C_6H_4)NO_2, (*E*)-NO_2, has been reported to display high molecular NLO responses, but shows no second harmonic generation (SHG) in the solid state [10,26]. Although it has been argued that the low efficiency in the bulk NLO response for (*E*)-NO_2 is due to its centrosymmetry, we did not find in the literature nor in the CSD the reported crystal structure for this compound. For this reason, we obtained single crystals of (*E*)-NO_2 and determined its molecular structure [27]. Compound (*E*)-NO_2 crystallizes in the centrosymmetric space group $P2_1/c$. As seen in Fig. 6, the molecule has an almost perfect coplanar arrangement between the ferrocenyl donor and the nitrophenyl moiety. The dimer pairs adopt a head-to-tail (DAAD) alignments in which the molecular dipoles mutually cancel each other out.

2.5. NLO properties

In this section, we summarize our most relevant results on NLO properties of our ferrocenyl push–pull complexes.

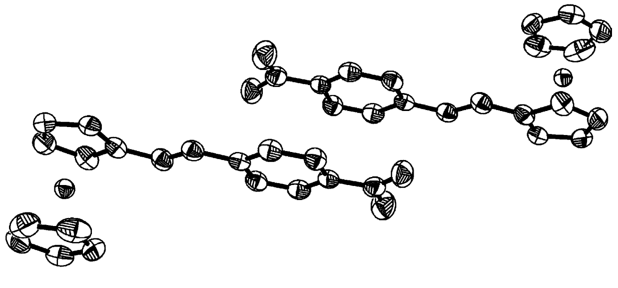

Fig. 6. View of the dimer pairs of (*E*)-NO_2 showing a head-to-tail (DAAD) alignment.

Table 3
NLO properties (hyperpolarizabilities, β) of some of the ferrocenyl complexes under study

Compound	β (10^{-30} esu)	Compound	β (10^{-30} esu)
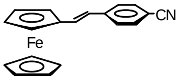	203	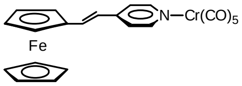	63
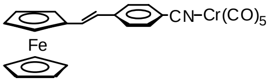	271	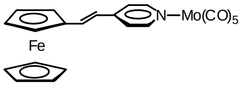	95
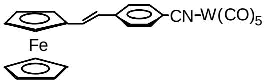	375	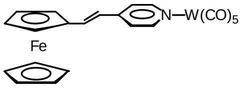	101
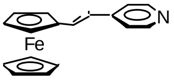	21	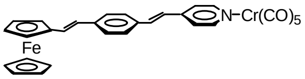	369
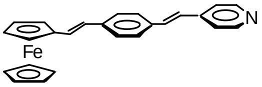	146	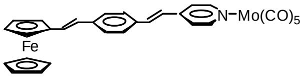	448
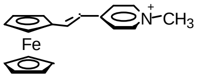	40[a]	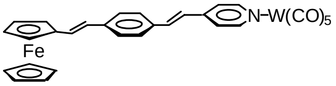	535
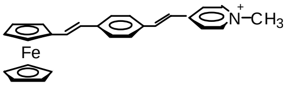	197[a]	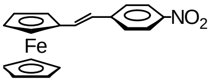	31 (EFISH)
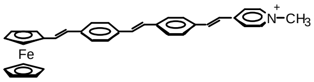	458[a]	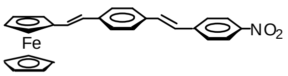	122
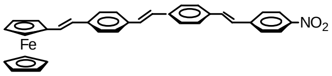	209	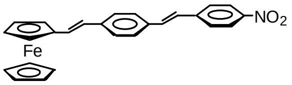	403

Values summarized from Refs. [17,27,32]. Calculated with respect to β of PNA in choloroform.

[a] Calculated with respect to β of PNA in acetone.

The aim of this work is to see whether there is a clear structure/properties relation in the compounds we have described, especially concerning their NLO outputs. In fact, this section is merely illustrating the work done by some other authors, who have studied these effects in a much deeper manner, and have described how organometallic and coordination chemistry can offer a very large variety of NLO structures in relation to the metal configuration, oxidation state, spin state, etc. Metal complexes can satisfy the very different demands of second-order NLO materials such as being switchable, tuneable, and having multi-dimensional NLO properties, depending on the subtle interplay of structure–property relationships [10,25,28].

All the compounds were measured by the hyper-Rayleigh scattering (HRS) technique [29]. The hyperpolarizabilities β for the most representative compounds are reported in Table 3. The neutral compounds were measured in chloroform, while acetone was used for the ionic methylpyridinium compounds due to their low solubility in the former solvent. It has been shown, that both the MLCT and the $\pi-\pi^*$ transitions lead to changes in β [30] so the two-level model may not be appropriate when considering metallocenes and we have not estimated the static hyperpolarizability values.

Some important structure–property relationships can be derived from the NLO values. As we can see in Table 3, several factors can affect the NLO response (β) of our complexes.

2.5.1. Electron-accepting group

The nature of the electron-accepting group in the push–pull complex has a clear effect on the NLO response of the compound. For similar conjugated chain lengths, the β values seem to follow a decreasing trend in the order $NO_2 > CN >$ pyr, thus reflecting that the higher electron-accepting character of the terminating moiety the higher NLO response.

The metal carbonyl moieties enhance the push–pull character compared to the pyridyl and nitrile uncoordinated species and even to the methyl-pyridinium compounds, as reflected by the higher β values observed. The β value increases when we change the metal, in the order W > Mo > Cr, probably due to the decrease in the Pauling electronegativity in the same direction and to the higher back donation capability of W compared to Cr and Mo. However, this point has to be considered as a crude estimation since hyperporalizabilities of organometallic push–pull complexes often exhibit significant solvent polarity dependence, thus enhancing β when the polarity increases (the measurements of the cationic species have been carried out in acetone, whilst neutral compounds were measured in $CHCl_3$). In this sense, it is observed that the stronger acceptor (cationic CH_3 terminated complexes) would not lead to the largest nonlinearities. This observation is rather surprising, although long π-chained complexes with better acceptors do not necessarily show higher nonlinear responses [31].

2.5.2. Chain lengthening

As expected, the increase in the conjugation length by *n* multiple bonds results in a rather dramatic increase in the β values, as seen for the methyl-pyridinium compounds (*E*)-*N*-CH_3, (*E*,*E*)-*N*-CH_3 and (*E*,*E*,*E*)-*N*-CH_3 (Table 3). A similar trend is observed for the neutral pyridyl complexes and for the NO_2 terminated complexes, although different increases in the β values are observed for each vinylene-phenylene unit added on the three series of complexes (-pyr, -pyr-$M(CO)_5$, and -NO_2).

According to theoretical calculations, a linear dependence between β and the length of the conjugated chain must not be expected [33]. In extended conjugated systems, the number of excited states contributing to β increases upon chain lengthening [34]. In an effort to quantify the NLO dependence with the chain length, Jayaprakash et al. found that the equation $\beta = an^b$ (where *a* and *b* are constant values and *n* the number of double bonds) [35] gives a good correlation for their compounds. Although a limited data are available for our compounds, we compared the different *b* values obtained using the same relationship. We found that the exponent *b* is 2.3 for the methyl-pyridinium complexes and 2.8 for the uncoordinated neutral pyridyl ones. For the metal carbonyl-substituted compounds, the values are 2.6, 2.2 and 2.4 for Cr, Mo, and W, respectively. For the NO_2 terminated complexes *b* is 3.6. These values are considerably higher than those obtained by Jayaprakash et al. in their study [35], showing that these seem to highly depend on the nature of the electron-accepting fragment, although in an apparently random manner.

2.5.3. Z/E configuration

We observe (Table 3) that the loss of conjugation is also reflected in a spectacular decrease in hyperpolarizability. This effect is particularly observed if we compare the β values for (*E*,*E*)-NO_2 with (*E*,*Z*)-NO_2 and (*E*,*E*,*Z*)-NO_2 complexes.

In general, we observe that electrochemical and spectroscopic studies give a good idea of the trends in NLO behavior in a series of similar complexes. In this sense, we always observe that maintaining the electron-accepting and electron-donating groups, chain lengthening promotes a bathochromic shift of the $\pi-\pi^*$ band, reduction of the redox potential, and an enhancement of the NLO response. These results confirm that the ferrocenyl derivatives follow the same qualitative design rules that have evolved for π-electron organic chromophores. However, our attempts to make quantitative predictions or good correlations between these physical properties and the hyperpolarizability values failed, probably due to the increase in the number of excited states contributing to β upon chain lengthening, thus making simple models to interpret the experimental data (such as the two-level model) poor approximations.

3. Compounds with linked ferrocenes

One of the richest areas of metallocene chemistry has been that of linked metallocenes [3]. Much of the interest in these species is concerned with the interaction between metal centers. When two or more ferrocenyl fragments are connected to obtain compounds with linked ferrocenes, many interests are envisaged, since intermetallic electronic communication affords a wide range of new applications. Many studies have been made during the last decade, regarding intramolecular electron-exchange reactions [3–6] and the number of papers devoted to describe the synthesis and electronic properties of new polymetallocenyl compounds has grown enormously in the last few years [5,8,36,37].

In this section, we describe the synthetic procedures and the physical properties of several conjugated bis-ferrocenyl compounds with end-capped pyridine and nitrile groups. Special attention is paid to the molecular structures and the electrochemistry of the described complexes.

3.1. Preparation of the complexes

Scheme 5 shows the general procedure for the synthesis of our linked bis-ferrocenyl complexes of the (Fc, Fc)-X type. The synthetic procedure is based on the Wittig olefination method, starting from ferrocene-1,1′-bis-carboxaldehyde. Since *E*-type isomers have shown higher efficiency for electronic coupling than the *Z*-type, we tried to optimize the preparation of the *E*-type isomers. In this sense, only the preparation of compounds (*E*)-(Fc, Fc)-CHO and (*E*,*E*)-(Fc, Fc)-NO_2 afforded a mixture of the corresponding *E*/*Z* isomers which could be easily separated. Furthermore, the *Z* isomers were quantitatively converted to the *E* homologues by treatment with I_2 in refluxing toluene. The preparation of compounds (*E*,*E*)-(Fc, Fc)-CN and (*E*,*E*)-(Fc, Fc)-pyr yielded the *E* isomers as the only isolable species.

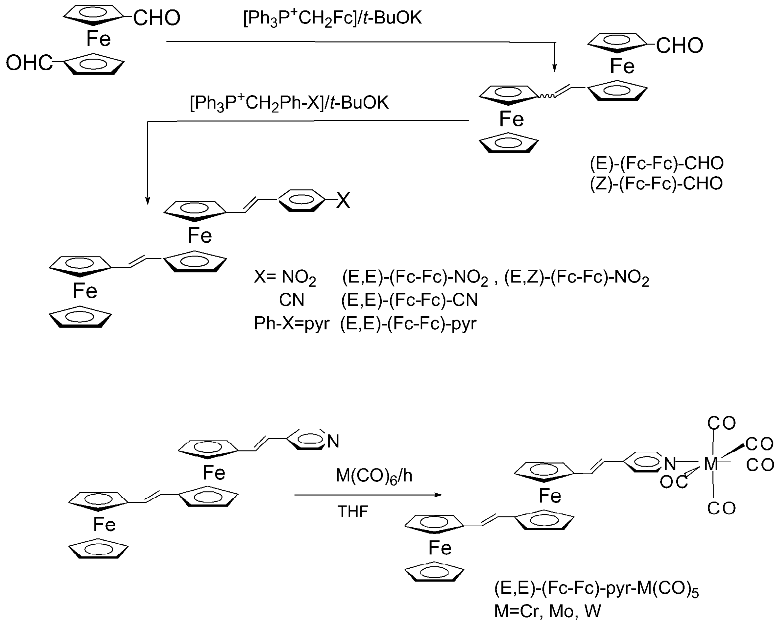

Scheme 5.

The coordination capabilities of the end-capped pyridine (*E*,*E*)-(Fc, Fc)-pyr, and nitrile, (*E*,*E*)-(Fc, Fc)-CN, bis-ferrocenyl complexes, allowed us to obtain the trimetallic species (*E*,*E*)-(Fc, Fc)-CN-M(CO)$_5$, and (*E*,*E*)-(Fc, Fc)-pyr-M(CO)$_5$ (M = Cr, Mo, W), by reacting the ligands with (THF)M(CO)$_5$ which was photochemically generated in situ (Scheme 5).

3.2. Molecular structure of the complexes

1,1′-Bis-substituted-ferrocenyl compounds offer a good opportunity to assess the impact of electronic and steric factors affecting the ferrocenyl disposition of the ancillary ligands of the ferrocene. In ferrocenyl complexes, it has been reported that two molecular motions relieve steric strain: [1] (i) the rotation from an eclipsed to a staggered disposition of the two Cp rings, and (ii) their tilting from a parallel disposition.

For compounds (*E*,*E*)-(Fc, Fc)-pyr-M(CO)$_5$ (M = Cr, Mo, W), there is a very similar geometrical arrangement in the molecular disposition of the molecules (see Figs. 7 and 8). The iron distances to the Cp rings and the Cp(C–C) distances and angles lie in the expected range. In all the cases that we have studied, the complexes show a perfect eclipsed disposition of the Cp rings in all the ferrocene units, and a slightly tilting angle can be observed between the two Cp rings of every Fc unit. As seen in some of the 1,1′-bis-substituted ferrocenyl complexes that we [38] and others [39,40] have reported so far, all these complexes adopt the sterically more hindered *syn* conformation, in a parallel disposition of the ancillary ligands in which intramolecular π-stacking may be having some effect. In the case of the complex (*E*)-(Fc, Fc)-CHO (Fig. 9), where π-stacking is not possible, the *syn* conformation is also observed, this indicates that packing effects may be having a more important effect in the steric disposition of the molecule in the

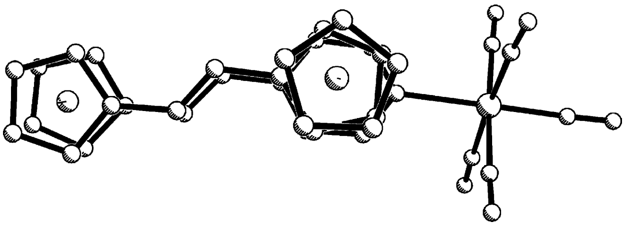

Fig. 7. Molecular structure for compound (*E*,*E*)-(Fc, Fc)-pyr-Mo(CO)$_5$, {(*E*,*E*)-(η^5-C_5H_5)Fe(η^5-C_5H_4)(CH=CH)(η^5-C_5H_4)Fe(η^5-C_5H_4)(CH=CH)PyMo(CO)$_5$}. Hydrogen atoms have been omitted for clarity [42].

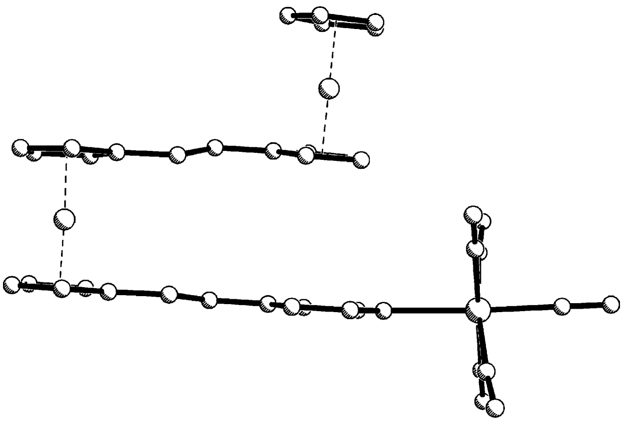

Fig. 8. Molecular structure and atomic labeling scheme for (*E*,*E*)-(Fc, Fc)-pyr-Cr(CO)$_5$, {(*E*,*E*)-(η^5-C_5H_5)Fe(η^5-C_5H_4)(CH=CH) (η^5-C_5H_4)Fe (η^5-C_5H_4)(CH=CH)PyCr(CO)$_5$}, with 50% displacement ellipsoids. The two molecules per asymmetric unit are shown. Hydrogen atoms have been omitted for clarity [42].

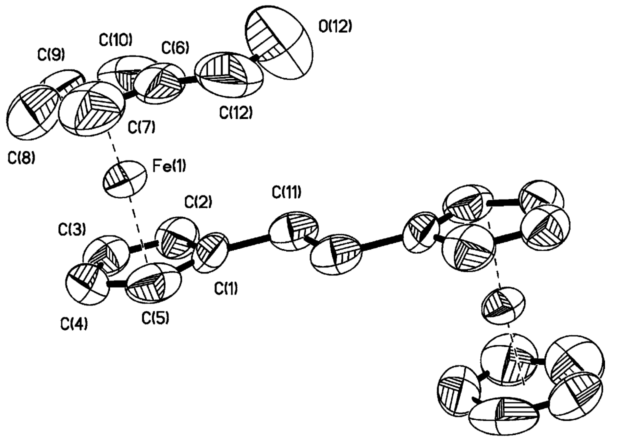

Fig. 9. Molecular structure and atomic labeling scheme for (*E*)-(Fc, Fc)-CHO, {(*E*)-(η^5-C_5H_5)Fe(η^5-C_5H_4)(CH=CH)(η^5-C_5H_4)Fe(η^5-C_5H_4)CHO} [42].

crystal structure. In this sense, Lee et al. have reported a study in which the eclipsed/staggered conformation of 1,1′-bis(ethenyl-4-pyridine)ferrocene is controlled by cocrystallization in various solvents [40]. This effect, together with the different conformations that 1,1′-bis-ferrocenyl complexes may adopt upon oxidation [41] make ferrocene behave as a ‘hinge-like’ compound, which interesting applications can be derived.

The orientation of the coordinated pyridyl rings with respect to the metal-carbonyl fragments is defined by the angles between the pyridyl plane and the plane defined by M (M = Cr, Mo, Cr) and three coplanar carbon atoms of the carbonyl ligands. In this regard, the pyridyl plane in (*E*,*E*)-(Fc, Fc)-pyr-Cr(CO)$_5$ is at an angle of 44.6° to the Cr(1)-C(30)-C(33)-C(34) mean plane, this angle being 66.1° and 44.7° for (*E*,*E*)-(Fc, Fc)-pyr-W(CO)$_5$ and (*E*,*E*)-(Fc, Fc)-pyr-W(CO)$_5$, respectively. M(dπ)–pyridine(π*) back bonding would be maximized when these angles are 0° or 90°. In our case, the carbonyl ligands adopt a quasi-staggered disposition with respect to the pyridine fragment (specially in the cases of (*E*,*E*)-(Fc, Fc)-pyr-Cr(CO)$_5$ and (*E*,*E*)-(Fc, Fc)-pyr-W(CO)$_5$, where the angle is practically equal to the idealized staggered disposition, 45°), so minimizing the steric interactions. The expected *trans* influence is present, with the M–C bonds *trans* to the pyridine ligand (Cr, 1.84 Å; Mo, 1.95 Å; W, 1.97 Å) being significantly shorter than the other M–C bonds (Cr, 1.90 Å; Mo, 2.05 Å; W, 2.02 Å). These results are in good agreement with the features of the molecular structures reported by Sakanishi et al. for other related ferrocenyl-pyridyl ligands coordinated to Cr(CO)$_5$ [43].

3.3. *Electrochemistry*

Electrochemical techniques have been the most widely used tools to investigate metal–metal interactions in metallocene systems and also to evaluate the donor–acceptor electronic influence. Here, we have used cyclic voltammetry in order to evaluate the redox properties of the metal centers, the degree of interaction, and the effect of the acceptor moiety [42].

Fig. 10 shows three voltammograms corresponding to compounds (*E*)-(Fc, Fc)-CHO, (*E*,*E*)-(Fc, Fc)-NO_2 and (*E*,*E*)-(Fc, Fc)-pyr-Cr(CO)$_5$. As can be seen, the redox bands corresponding to the two ferrocenyl fragments, are very poorly influenced by the nature of the ancillary ligands. This is a general behavior for all the bis-ferrocenyl complexes in our study. Only in the case of the aldehyde complexes (*E*)-(Fc, Fc)-CHO and (*Z*)-(Fc, Fc)-CHO, the half-wave potentials of the ferrocenyl moieties show a clear positive shift compared with (*E*)-Fc-CH=CH-Fc, meaning some degree of electron transfer between the iron center and the electron-accepting aldehyde fragment. However, the half-wave potentials of the nitrile and pyridine derivatives with longer conjugated chains are similar to that shown for (*E*)-Fc-CH=CH-Fc indicating that the inclusion of the electron-accepting fragments (pyr, -CN), are somehow compensated by the delocalization of the charge along the longer conjugated system of the ligand, which makes oxidation easier.

Coordination of the neutral unit M(CO)$_5$, to the ferrocenyl nitrile and pyridine ligands, does not have any signif-

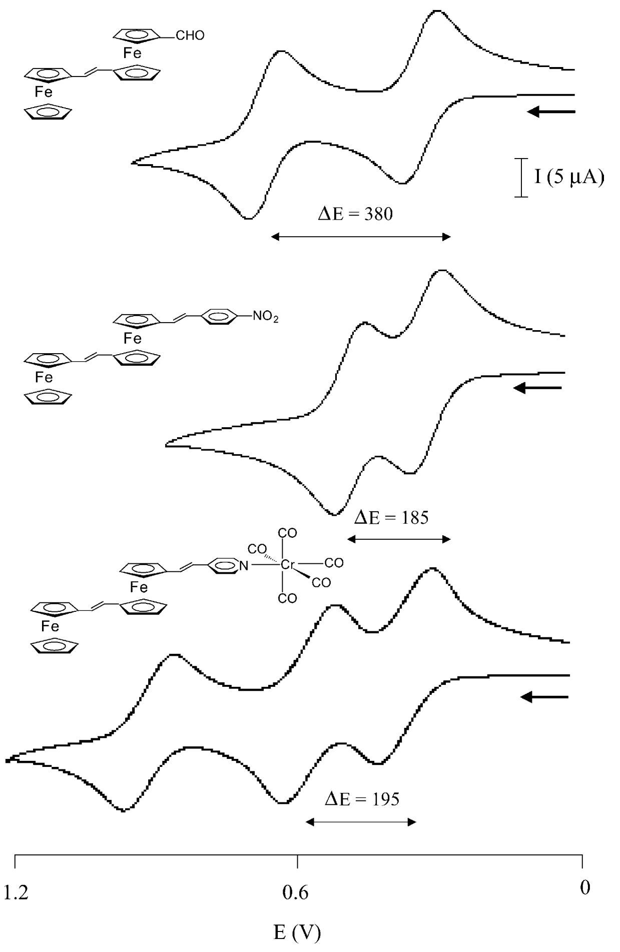

Fig. 10. Cyclic voltammograms (scan rate 100 mV s^{-1}) of (*E*)-(Fc, Fc)-CHO, (*E*,*E*)-(Fc, Fc)-NO_2, and (*E*,*E*)-(Fc, Fc)-pyr-Cr(CO)$_5$ [42].

icant effect on the redox potential of the ferrocene centers, compared to those of the pyridine and nitrile ligands. The oxidation potential of the third step ascribed to the metal-carbonyl fragment depends on the metal present, this being higher for the W complexes compared to the Cr and Mo complexes. This band is only reversible in the case were $Cr(CO)_6$ was used. This result is consistent with those studies reported before where chromium and tungsten ferrocenyl derivatives show quasi-reversible and complete irreversible oxidation waves, respectively [13,17,20,44].

The degree of separation or resolution of the two waves in the homobimetallic compounds, is a quasi-direct measure of the degree of interaction of these metals, although we have to take into account the intrinsic inequivalency of the two metal centers. The presence of two one-electron oxidations instead of one two-electron oxidation indicates a stabilization of the mixed valence species. The separation between the two oxidation potentials, was employed to calculate the comproportionation constant, K_c, from, the following equations:

$$(\mathrm{Fc^{II}, Fc^{II}}) + (\mathrm{Fc^{III}, Fc^{III}}) \overset{K_c}{\Leftrightarrow} 2(\mathrm{Fc^{III}, Fc^{II}}) \tag{1}$$

$$\Delta E = \Delta E_{1/2}(\mathrm{Fc^{III}, Fc^{III}}) - \Delta E_{1/2}(\mathrm{Fc^{III}, Fc^{II}}) \tag{2}$$

$$\Delta E\,(\mathrm{mV}) = 59.15(\log K_c) \quad \text{at}\, 298\,\mathrm{K} \tag{3}$$

This is a crude estimation of the interaction between the iron centers due to their geometrical inequivalence, but it gives us an approximate estimation of the electronic communication between the two metal centers. This approximation has also been used in some other examples in which the two metal centers were inequivalent, and even in cases in which the metals were different [37]. In any case, we are aware that the electronic communication between the redox centers must be less than that measured by the potential difference.

K_c values obtained by Eq. (3) lie in the range of the weakly connected class II mixed-valence complexes (ΔE, ca. 200 mV). The most interesting feature of this interaction between our diferrocenyl derivatives is the strong coupling observed for compounds (*E*)-(Fc, Fc)-CHO (ΔE = 380 mV) and (*Z*)-(Fc, Fc)-CHO (ΔE = 355 mV), especially when we compare these values to the ones published before. For example in the case of (*E*)-Fc-CH=CH-Fc the coupling constant is ca. 150 mV [45]. The coupling in (*E*)-(Fc, Fc)-CHO is larger than that of (*E*)-Fc-CH=CH-Fc, even in the case that we considered an intrinsic inequivalence of 60 mV, which is approximately the difference in the redox potentials of ferrocene (445 mV) and ferrocenealdehyde (500 mV).

4. Two-dimensional star-shaped compounds-metallodendrimers

Since Vögtle and coworkers obtained the first acyclic branched polyamines [46] dendrimer chemistry has attracted the interest of a large number of chemists, who mainly pursued new synthetic routes for the production of high molecular weight compounds with as many generations as possible. More recently, the interest in dendrimer chemistry, turned to the modification of the properties of dendritic compounds by either the introduction of internal or peripheral functionalities, as this can provide access to materials with potential magnetic, electronic, photo-optical or catalytical properties. The introduction of metal atoms into the structure of the dendrimer, has allowed the generation of a new type of molecules called *metallodendrimers* [47,48]. The inclusion of redox centers into the dendrimer wide-spreads the structural diversity and the properties of these materials. Many approaches have been used to introduce the metal centers into the dendrimer structure, but still we can see that the lack of systematic preparation procedures constitute the bottleneck of the study of this new type of materials.

Among all the metallodendrimers obtained until now, those containing ferrocene seem to have attracted a special attention [48–50] undoubtedly because ferrocene combines chemical versatility with high thermal and redox stability.

4.1. Preparation of the compounds

In the design of two-dimensional dendrimers, we considered that using ferrocenyl–vinyl-phenylene-derived dendrons would be a good starting point due to the planar configuration that they showed in their molecular structures (see previous sections). The convergent synthesis that we have proposed is based on the preparation of olefin-terminated dendrons, which can be coupled to halogen-containing cores by simple Heck coupling reactions.

As seen in Scheme 6, the general procedure for the preparation of the two-dimensional dendrons, is based in a combination of the Wittig and Heck coupling reactions. By this method, we were able to obtain olefin terminated first- and second-generation dendrons [$(Fc)_2$-CH=CH_2 and $(Fc)_4$-CH=CH_2] in good yields.

As the core for the preparation of our dendrimers, we first tried to use 1,3,5-tribromobenzene, since it gives excellent results in the Heck-coupling of ferrocenyl–vinylene [41]. The reaction of a three-fold excess of $(Fc)_2$-CH=CH_2 with 1,3,5-tribromobenzene yielded unambiguously a tetraferrocenyl complex indicating that only two dendrons bound to the core. Higher excesses of $(Fc)_2$-CH=CH_2 in the reaction procedure, higher amounts of catalyst or the use of higher temperatures, did not afford the three-fold coupled dendrimer. We believe that the reason for this is the coplanarity imposed by the extended conjugated system, clearly making the steric or ‘starburst’ limit of this two-dimensional dendrimer, already achieved in the first generation.

Since we believed that steric reasons were the only ones to blame for the failure in the synthesis of our hexaferrocenyl dendrimer, we decided to use compounds 1-Br_3 and 2-Br_6 as new cores. With these two compounds the steric strain is released because (i) the bromine atoms show a higher through space distance, and (ii) the less effective

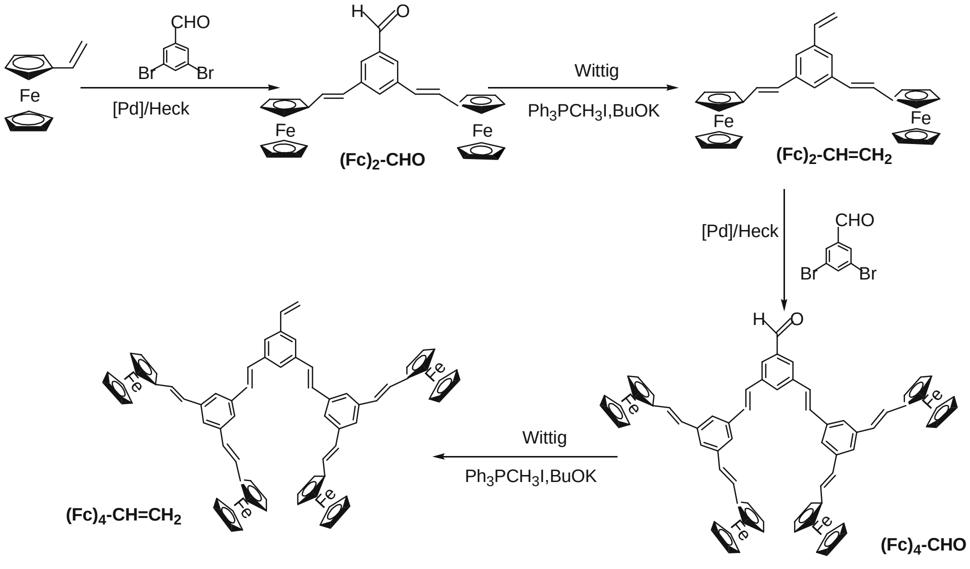

Scheme 6.

conjugation between the phenylene connections, affords a lower C–C rotation barrier which can break the coplanarity of the whole molecule, but the coplanarity of each individual branch should be maintained. Compound 2-Br_6 was obtained by Miller et al. [51] and was satisfactorily used in the preparation of a series of monodisperse organic dendrimers. By a similar method to that leading to 2-Br_6, we obtained 1-Br_3 in very high yield (ca. 80%) starting from commercially available 4-bromoacetophenone (Scheme 7).

The reaction of 1-Br_3 and 2-Br_6 with vinylferrocene, affords the preparation of three- and six-ferrocenyl containing dendrimers, 3-Fc_3 and 4-Fc_6 (Scheme 7). More interesting are the reactions of the first generation dendron $(Fc)_2$-$CH{=}CH_2$ with 1-Br_3 and 2-Br_6 yielding the dendrimers 5-Fc_6 and 6-Fc_{12} (Scheme 8). Although the ^{1}H and ^{13}C NMR spectra of the compounds are rather clean, the assignment of the signals for the more complicated compounds 5-Fc_6 and 6-Fc_{12} cannot be easily made due to the overlapping of the peaks corresponding to the olefin and aromatic hydrogens. However, the $^3J_{H-H}$ coupling of the olefin hydrogen atoms were in all cases very close to 16 Hz, which unambiguously confirms the all-*E* configuration of the complexes. The ^{1}H NMR spectra also shows the pattern of mono-substituted ferrocenyl compounds, this confirming the equivalence of the peripheral ferrocene units. The structure of the compounds 5-Fc_6 and 6-Fc_{12} was corroborated by fast atom bombardment mass spectroscopy (FAB-ms).

We were unsuccessful in obtaining good single crystals of the dendrimers, but we could resolve the crystal structure of the first generation dendrimer $(Fc)_2CH{=}CH_2$. Fig. 11 shows

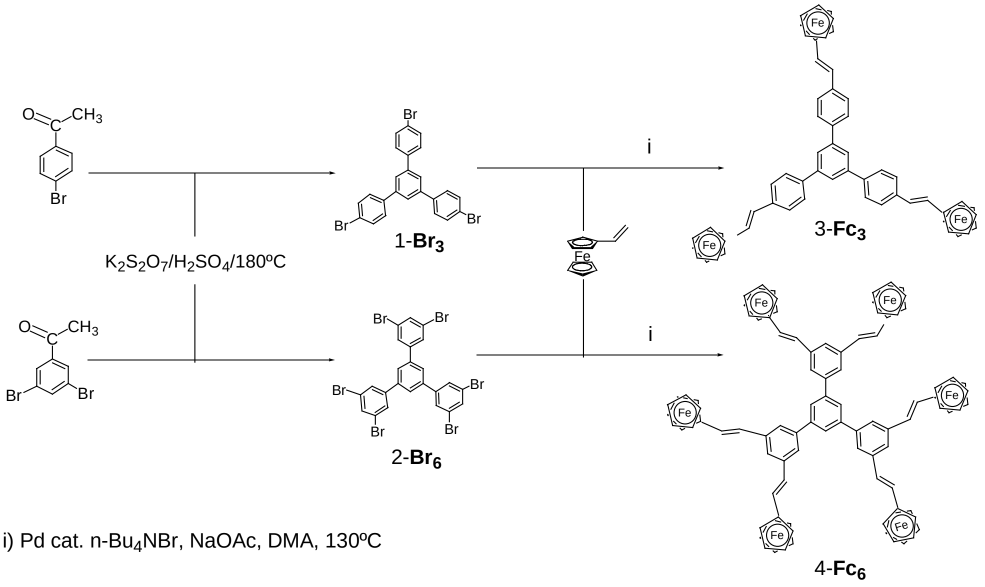

i) Pd cat. n-Bu_4NBr, NaOAc, DMA, 130ºC

Scheme 7.

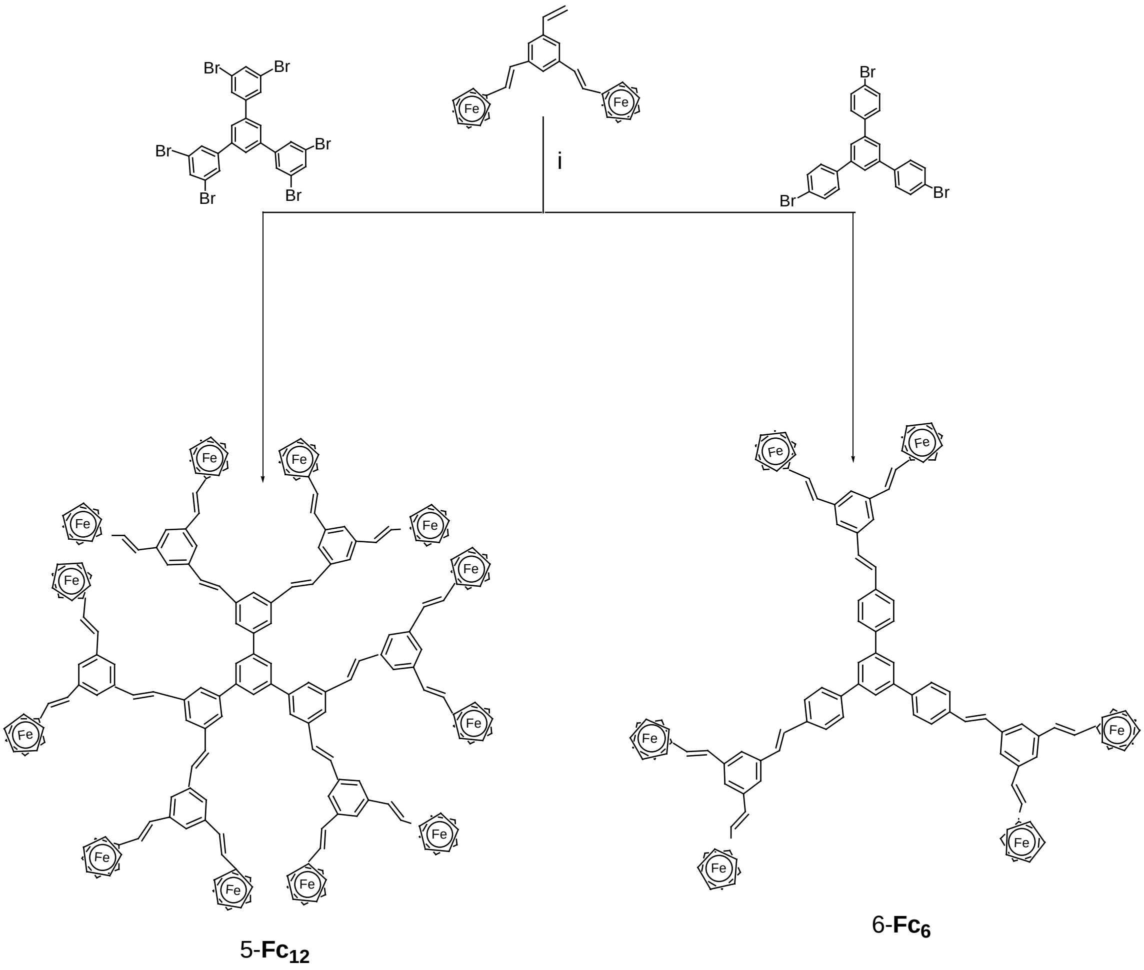

i) Pd cat. n-Bu$_4$NBr, NaOAc, DMA, 130ºC

Scheme 8.

the ORTEP diagram of $(Fc)_2CH=CH_2$ in two different perspectives. The most remarkable feature of this structure is that it shows an almost coplanar structure between the Cp, vinylene and phenylene units, as can be seen in Fig. 11b, confirming that the conjugation extends along the whole structure. We believe that the coplanar arrangement of the dendron may be extended to the whole structure of the dendrimers. This fact, implies that the structure of the dendrons be two-dimensional and the dendrimers should also probably be two-dimensional.

From the electrochemical data, we can observe that, in general, all the dendrimer type complexes described, show lower potentials than that shown for ferrocene (445 mV), probably due to their higher electron delocalization abilities. A cooperative electron-donating character of each ferrocenyl unit may be also contributing to this redox potential lowering. Compounds 3-Fc$_3$, 4-Fc$_6$, 5-Fc$_6$ and 6-Fc$_{12}$ show a unique reversible electron wave, this corresponding to the simultaneous oxidation of 3, 6, 6, and 12 ferrocene units, respectively. This result indicates that the ferrocenyl centers in each compound are essentially non-interacting. However, this result may also be interpreted as a consequence of fast heterogeneous electron-transfer kinetics. It has been suggested that one of the reasons for this observation may be due to the fast rotation of the dendrimer compared to the electrochemical timescale, so that all redox centers come close to the electrode within this timescale [50]. A similar effect was observed for the compound 1,3,5-tris(ferrocenylethenyl)benzene [41].

As previously reported for other ferrocenyl dendrimers [53] the redox behavior of the compounds 3-Fc$_3$, 4-Fc$_6$, 5-Fc$_6$ and 6-Fc$_{12}$ is marked by changes in solubility with the change in the oxidation state of ferrocene units. Whereas the anodic wave has a typical diffusional shape, a sharp cathodic stripping peak is observed, which indicates precipitation of the dendrimers onto the electrode upon oxidation.

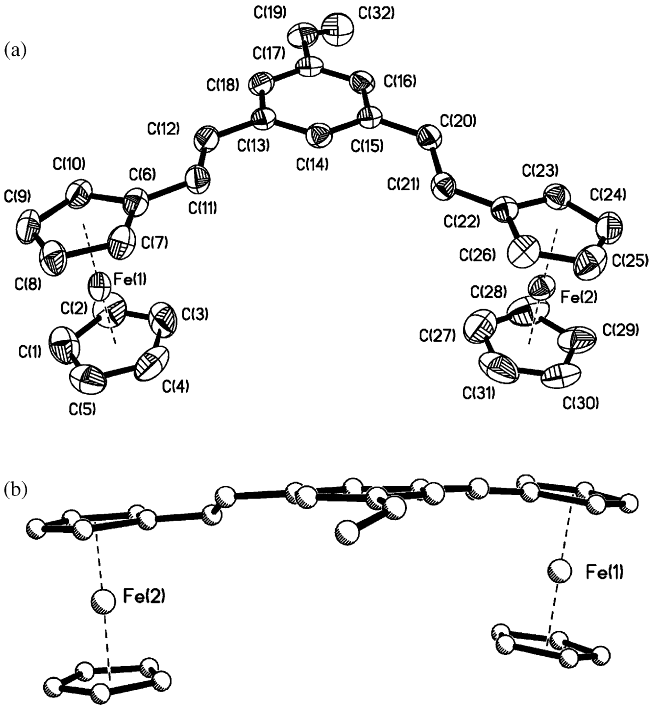

Fig. 11. Two perspectives of the molecular diagram of the first generation dendron $(Fc)_2CH=CH_2$, showing its coplanarity in panel (b) [52].

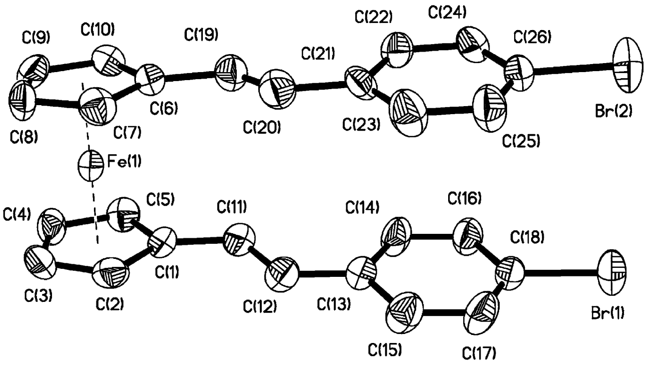

Fig. 12. Molecular diagram of (*E*,*E*)-1,1′-bis[*p*-bromophenyl-ethenyl]-ferrocene [42].

4.2. Other dendritic polyferrocenyl complexes

In the search of new polyferrocenyl complexes, we thought that 1,1′-(phenylene-ethenyl)bis-substituted ferrocenes could provide a new family of complexes with interesting structural and electronic properties. 1,1′-Bis-substituted ferrocenes are known to show interesting properties derived from what we have called ‘hinge-like’ structure [42,52]. In this sense, we synthesized (*E*,*E*)-1,1′-bis[*p*-bromophenyl-ethenyl]-ferrocene, as the core for a new series of oligoferrocenyl compounds. The synthesis of this new core was based on the conventional Wittig olefination method from 1,1′-bis-carboxaldehyde-ferrocene.

The crystal structures of the compounds (*E*,*E*)-1,1′-bis[*p*-bromophenyl-ethenyl]-ferrocene and its (*E*,*Z*) analogue were determined by means of X-ray diffractometry. Fig. 12 shows the ORTEP diagram for the (*E*,*E*) isomer. The most remarkable feature is that it shows an almost coplanar structure between the Cp, vinylene and phenylene units, confirming that the conjugation is extended along all the structure. As described in the previous sections for other ferrocenyl complexes, the Cp rings adopt an eclipsed conformation, with the two ancillary ligands in a *syn* conformation.

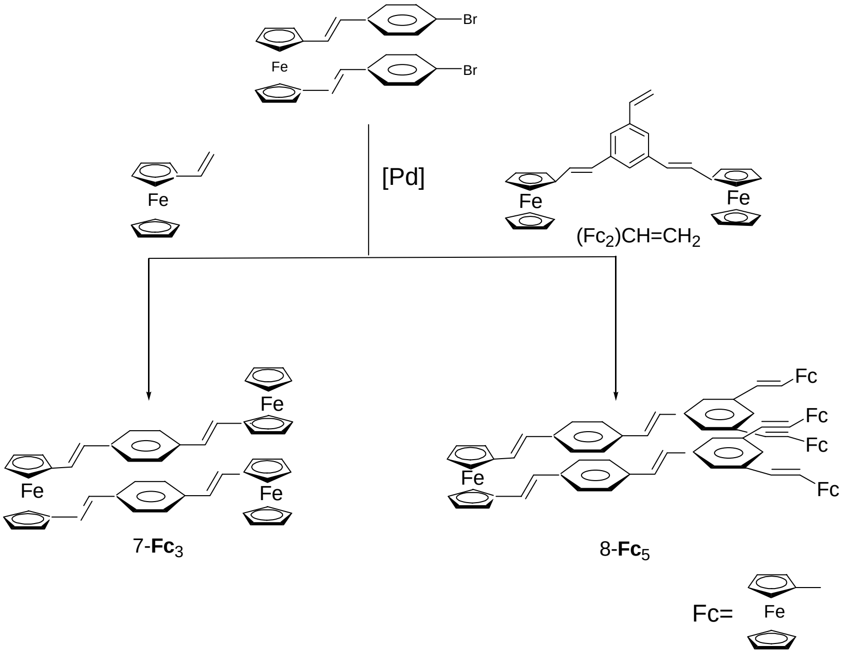

Scheme 9.

This observation has been reported by some other authors [38–40,42].

As mentioned before, (*E,E*)-1,1′-bis[*p*-bromophenyl-ethenyl]-ferrocene was used as the core for the synthesis of several oligo-ferrocenyl complexes. The palladium catalyzed reaction with vinylferrocene afforded the trisferrocenyl complex 7-Fc_3 in very high yield (Scheme 9). By following a similar procedure, the reaction of $(Fc_2)CH{=}CH_2$ with (*E,E*)-1,1′-bis[*p*-bromophenyl-ethenyl]-ferrocene afforded the pentaferrocenyl complex 8-Fc_5 (Scheme 9) in high yield. Compounds 7-Fc_3 and 8-Fc_5 were fully characterized by conventional methods. Although we failed to obtain good single crystals suitable for X-ray diffraction studies, we consider that it is highly probable that the structures of these two complexes also show a high degree of coplanarity. If we also consider the ability of 1,1′-bis-substituted ferrocenyl complexes to display *syn* conformations, we believe that a fluxional equilibrium of all the possible rotamers must be present in solution of compounds 7-Fc_3 and 8-Fc_5.

In cyclic voltammetry, the tri- and penta-ferrocenyl complexes 7-Fc_3 and 8-Fc_5 display two reversible peaks corresponding to the central ferrocene and the equivalent terminal ferrocenyl units. The lower potential waves correspond to a two-electron oxidation process in compound 7-Fc_3 and four-electron in the case of compound 8-Fc_5 imply that the oxidation of the terminal units occurs at a lower potential than the central bis-substituted ferrocene. It can be shown [54] that in a molecule with *n* noninteracting equivalent redox centers, in an electrochemical experiment, one should observe a separation, ΔE, of $(RT/F)\ln 2^n$ between the first and the last redox events within the equivalent redox centers. This would imply that, in our case, compound 7-Fc_3, with two noninteracting redox centers, should display a peak separation of 36 mV for the two terminal ferrocenyl units. In the case of compound 8-Fc_5, the peak separation of the four noninteracting peripheral units would be of 72 mV. Both numbers are rather small separations to be resolvable in routine electrochemical experiments. When we study the peak separation between the peripheral and the central ferrocenyl units, we observe that this is rather large for both compounds 7-Fc_3 (300 mV) and 8-Fc_5 (400 mV). The presence of two one-electron oxidation instead of one two-electron oxidations indicates a stabilization of the mixed valence species. In any case, we are aware that the electronic communication between the redox centers must be less than that suggested by the potential difference, due to the intrinsic inequivalence of the iron centers implied in the two redox processes.

The half-wave peak separations in 7-Fc_3 and 8-Fc_5 prompted us to obtain the mixed-valence complexes 7-$Fc_3{}^{2+}$ and 8-$Fc_5{}^{4+}$ by oxidizing the neutral complexes with an excess of ferrocenium-hexafluorophosphate as an oxidant. The resulting products were analyzed by electrospray mass spectroscopy. This showed major peaks corresponding to the dicationic species for 7-Fc_3 and tetracationic for 8-Fc_5. 7-Fc_3 and 8-Fc_5 can also be oxidized to the 7-$Fc_3{}^{3+}$ and 8-$Fc_5{}^{5+}$ species by using a stronger oxidant such as $NOBF_4$. We strongly believe that the oxidized compounds must display interesting structural features, such as a fully expanded *anti* conformation in order to avoid electrostatic repulsions of the peripheral cationic centers. In fact, the change in conformation suffered by this complexes upon oxidation must have important applications in the design of new molecular switches.

5. Conclusions

From the study of the molecular structures, electronic spectra and cyclic voltammetry of a series of phenyl-ethenyl complexes of ferrocene, we have tried to rationalize some of their physical properties. In general, we have observed that, for mono-dimensional oligomers, electrochemical, and spectroscopic studies give a good idea of the trends in NLO behavior in a series of similar compounds. In this sense, we always observe that while maintaining the same electron-accepting and electron-donating groups, chain lengthening promotes a bathochromic shift of the $\pi-\pi^*$ band, reduction of the redox potential, and an enhancement of the NLO response. This behavior confirms that the ferrocenyl derivatives that we have studied, follow the same qualitative rules that have evolved for π-electron organic chromophores.

A new family of linked ferrocenyl complexes has been described, showing interesting electrochemical properties, specially regarding the strong coupling observed for the vinyl-connected bis-ferrocenes. The interaction between the ferrocenyl units depends on the substituents on the ferrocene. Interestingly, the molecular structures of these compounds present the more sterically hindered eclipsed conformation.

Some dendritic two-dimensional complexes have been obtained and their electronic properties have been studied. According to the molecular structure of the conjugated dendrons, the dendrimers described must show three planar branches, the coplanarity only being disrupted at the central core. We have established that Pd-mediated C=C bond formation is an effective method for the synthesis of conjugated ferrocenyl dendrimers and can be extended to the design of higher generation dendrimers.

Acknowledgements

We gratefully acknowledge financial support from the DGESIC (MAT2002-04421-C02-01) and Bancaixa (P1.1B2001-03).

References

[1] A. Togni, T. Hayashi, Ferrocenes, VCH Verlagsgesellschaft mbH, Weinheim, Germany, 1995.
[2] N.J. Long, Metallocenes, 1st ed., London, 1997.

[3] S. Barlow, D. O'Hare, Chem. Rev. 97 (1997) 637.

[4] M. Kurosawa, T. Nankawa, T. Matsuda, K. Kubo, M. Kurihara, H. Nishihara, Inorg. Chem. 38 (1999) 5113;
T. Horikoshi, K. Kubo, H. Nishihara, J. Chem. Soc. Dalton Trans. (1999) 3355;
T.-Y. Dong, P.-H. Ho, X.-Q. Lai, Z.-W. Lin, K.-J. Lin, Organometallics 19 (2000) 1096;
T.Y. Dong, C.K. Chang, C.H. Cheng, K.J. Lin, Organometallics 18 (1999) 1911.

[5] Y.J. Chen, D.-S. Pan, C.-F. Chiu, J.-X. Su, S.J. Ling, K.S. Kwan, Inorg. Chem. 39 (2000) 953.

[6] N.J. Long, A.J. Martin, R. Vilar, A.J.P. White, D.J. Williams, M. Younus, Organometallics 18 (1999) 4261.

[7] E. Stankovic, S. Toma, R. Van Boxel, I. Asselberghs, A. Persoons, J. Organomet. Chem. 637 (2001) 426;
D. Prim, A. Auffrant, Z.F. Plyta, J.P. Tranchier, F. Rose-Munch, E. Rose, J. Organomet. Chem. 624 (2001) 124;
R. Frantz, F. Carre, J.O. Durand, G.F. Lanneau, New J. Chem. 25 (2001) 188;
S. Creager, C.J. Yu, C. Bamdad, S. O'Connor, T. MacLean, E. Lam, Y. Chong, G.T. Olsen, J.Y. Luo, M. Gozin, J.F. Kayyem, J. Am. Chem. Soc. 121 (1999) 1059;
J.T. Lin, J.J. Wu, C.-S. Li, Y.S. Wen, K.-J. Lin, Organometallics 15 (1996) 5028;
V. Alain, M. Blanchard-Desce, C.-T. Chen, S.R. Marder, A. Fort, M. Barzoukas, Synth. Met. 81 (1996) 133;
A. Green, M.R. Bryce, A.S. Batsanov, J.A.K. Howard, J. Organomet. Chem. 590 (1999) 180;
H. Schottenberger, K. Wurst, M.R. Buchmeiser, J. Organomet. Chem. 584 (1999) 301;
H. Wong, T. Meyer-Friedrichsen, T. Farrell, C. Mecker, J. Heck, Eur. J. Inorg. Chem. (2000) 631.

[8] M. Bochmann, J.J. Lu, R.D. Cannon, J. Organomet. Chem. 518 (1996) 97.

[9] S. Barlow, H.E. Bunting, C. Ringham, J.C. Green, G.U. Bublitz, S.G. Boxer, J.W. Perry, S.R. Marder, J. Am. Chem. Soc. 121 (1999) 3715.

[10] N.J. Long, Angew. Chem. Int. Ed. Eng. 34 (1995) 21.

[11] A. Hradsky, B. Bildstein, N. Schuler, H. Schottenberg, P. Jaitner, K.-H. Ongania, K. Wurst, J.-P. Launay, Organometallics 16 (1997) 392.

[12] G.G.A. Balavoine, J.C. Daran, G. Iftime, P.G. Lacroix, E. Manoury, J.A. Delaire, I. Maltey-Fanton, K. Nakatani, S. Di Bella, Organometallics 18 (1999) 21.

[13] M. Bhadbhade, A. Das, J.C. Jeffery, J.A. McCleverty, J.A.N. Badiola, M.D. Ward, J. Chem. Soc. Dalton Trans. (1995) 2769.

[14] H.E. Bunting, M.L.H. Green, S.R. Marder, M.E. Thompson, D. Bloor, P.V. Kolinsky, R.J. Jones, Polyhedron 11 (1992) 1489.

[15] J.C. Calabrese, L.-T. Cheng, J.C. Green, S.R. Mader, W. Tam, J. Am. Chem. Soc. 113 (1991) 7227.

[16] A. Houlton, J.R. Miller, J. Silver, N. Jassim, M.J. Ahmet, T.L. Axon, D. Bloor, G.H. Cross, Inorg. Chim. Acta 205 (1993) 67.

[17] J. Mata, S. Uriel, E. Peris, R. Llusar, S. Houbrechts, A. Persoons, J. Organomet. Chem. 562 (1998) 197.

[18] J. Boutagy, R. Thomas, Chem. Rev. 74 (1974) 87;
W. Wadsworth, W.D. Emmons, J. Am. Chem. Soc. 83 (1961) 1733.

[19] H. Wong, T. Meyer-Friedrichsen, T. Farrell, C. Mecker, J. Heck, Eur. J. Inorg. Chem. (2000) 631.

[20] J.A. Mata, E. Falomir, R. Llusar, E. Peris, J. Organomet. Chem. 616 (2000) 80.

[21] J.A. Mata, S. Uriel, R. Llusar, E. Peris, Organometallics 19 (2000) 3797.

[22] H. Nock, H. Schottenberg, J. Org. Chem. 58 (1993) 7045;
A. Togni, G. Rihs, Organometallics 12 (1993) 3368.

[23] D.R. Kanis, M.A. Ratner, T.J. Marks, J. Am. Chem. Soc. 114 (1992) 10338.

[24] R.P. Hsung, C.E.D. Chidsey, L.R. Sita, Organometallics 14 (1995) 4808.

[25] I.R. Whittall, A.M. McDonagh, M.G. Humphrey, M. Samoc, Organometallic Complexes in Nonlinear Optics. I: Second-Order Nonlinearities, vol. 42, Academic Press Inc., San Diego, 1998.

[26] M.L.H. Green, S.R. Marder, M.E. Thompson, J.A. Bandy, D. Bloor, P.V. Kolinsky, R.J. Jones, Nature 330 (1987) 360.

[27] J.A. Mata, E. Peris, I. Asselberghs, R. Van Boxel, A. Persoons, New J. Chem. 25 (2001) 299.

[28] S. Di Bella, Chem. Soc. Rev. 30 (2001) 355;
J. Heck, S. Dabek, T. Meyer-Friedrichsen, H. Wong, Coord. Chem. Rev. 192 (1999) 1217.

[29] K. Clays, A. Persoons, Rev. Sci. Instrum. 63 (1992) 3285.

[30] M. Stahelin, D.M. Burland, J.E. Rice, Chem. Phys. Lett. 191 (1992) 245.

[31] S.R. Marder, C.B. Gorman, B.G. Tiemann, L.T. Cheng, J. Am. Chem. Soc. 115 (1993) 3006.

[32] J.A. Mata, E. Peris, S. Uriel, R. Llusar, I. Asselberghs, A. Persoons, Polyhedron 20 (2001) 2083;
J.A. Mata, E. Peris, I. Asselberghs, R. Van Boxel, A. Persoons, New J. Chem. 25 (2001) 1043.

[33] S. Ramasesha, P.K. Das, Chem. Phys. 145 (1990) 343;
I.D.L. Albert, P.K. Das, S. Ramasesha, Chem. Phys. Lett. 168 (1990) 454.

[34] C.B. Gorman, S.R. Marder, Proc. Natl. Acad. Sci. U.S.A. 90 (1993) 11297.

[35] K.N. Jayaprakash, P.C. Ray, I. Matsuoka, M.M. Bhadbhade, V.G. Puranik, P.K. Das, H. Nishihara, A. Sarkar, Organometallics 18 (1999) 3851.

[36] P. Zanello, G. Opromolla, M. Herberhold, H.D. Brendel, J. Organomet. Chem. 484 (1994) 67;
K.H. Pannell, V.V. Dementiev, H. Li, F. Cervanteslee, M.T. Nguyen, A.F. Diaz, Organometallics 13 (1994) 3644;
C.Y. Duan, Y.P. Tian, Z.H. Liu, X.Z. You, T.C.W. Mak, J. Organomet. Chem. 570 (1998) 155;
M.J. MacLachlan, J. Zheng, A.J. Lough, I. Manners, Organometallics 18 (1999) 1337;
K.R.J. Thomas, J.T. Lin, Y.S. Wen, Organometallics 19 (2000) 1008.

[37] J.Y. Chen, C.-H. Kao, S.J. Lin, C.-C. Tai, K.S. Kwan, Inorg. Chem. 39 (2000) 189.

[38] J.A. Mata, E. Peris, R. Llusar, S. Uriel, M.P. Cifuentes, M.G. Humphrey, M. Samoc, B. Luther-Davies, Eur. J. Inorg. Chem. (2001) 2113.

[39] A. Togni, M. Hobi, G. Rihs, G. Rist, A. Albinati, P. Zanello, D. Zech, H. Keller, Organometallics 13 (1994) 1224.

[40] I.S. Lee, Y.K. Chung, J. Mun, C.S. Yoon, Organometallics 18 (1999) 5080.

[41] A. Peruga, J.A. Mata, D. Sainz, E. Peris, J. Organomet. Chem. 637 (2001) 191.

[42] J.A. Mata, E. Peris, J. Chem. Soc. Dalton Trans. (2001) 3634.

[43] S. Sakanishi, D.A. Bardwell, S. Couchman, J.C. Jeffery, J.A. McCleverty, M.D. Ward, J. Organomet. Chem. 528 (1997) 35.

[44] L.K. Yeung, J.E. Kim, Y.K. Chung, P.H. Rieger, D.A. Sweigart, Organometallics 15 (1996) 3891;
I.P. Gubin, V.S. Khabdkarova, J. Organomet. Chem. 22 (1970) 449.

[45] A.-C. Ribou, J.P. Launay, M.L. Sachtleben, H. Li, C.W. Spangler, Inorg. Chem. 35 (1996) 3735.

[46] E. Buhleier, W. Wehner, F. Vögtle, Synthesis (1978) 155.

[47] G.R. Newkome, E.F. He, C.N. Moorefield, Chem. Rev. 99 (1999) 1689;
I. Cuadrado, M. Moran, C.M. Casado, B. Alonso, J. Losada, Coord. Chem. Rev. 195 (1999) 395;
D. Astruc, Acc. Chem. Res. 33 (2000) 287;
L. Lindoy, Coord. Chem. Rev. 174 (1998) 327;
V. Balzani, S. Campagna, G. Denti, A. Juris, S. Serroni, M. Venturi, Acc. Chem. Res. 31 (1998) 26.

[48] C.M. Casado, I. Cuadrado, M. Moran, B. Alonso, B. Garcia, B. Gonzalez, J. Losada, Coord. Chem. Rev. 186 (1999) 53.

[49] J. Ruiz, E. Alonso, J.C. Blais, D. Astruc, J. Organomet. Chem. 582 (1999) 139;
O. Briel, A. Fehn, W. Beck, J. Organomet. Chem. 578 (1999) 247;
D. Vos, A. Salmon, H.G. Stammler, B. Neumann, P. Jutzi, Organometallics 19 (2000) 3874;
C. Valerio, F. Moulines, J. Ruiz, J.C. Blais, D. Astruc, J. Org. Chem. 65 (2000) 1996;
C.M. Cardona, T.D. McCarley, A.E. Kaifer, J. Org. Chem. 65 (2000) 1857;
K.W. Poon, Y. Yan, X.Y. Li, D.K.P. Ng, Organometallics 18 (1999) 3528;
B. Garcia, C.M. Casado, I. Cuadrado, B. Alonso, M. Moran, J. Losada, Organometallics 18 (1999) 2349;
C.M. Casado, I. Cuadrado, W. Moran, B. Alonso, M. Barranco, J. Losada, Appl. Organomet. Chem. 13 (1999) 245;
C.M. Casado, I. Cuadrado, B. Alonso, M. Moran, J. Losada, J. Electroanal. Chem. 463 (1999) 87;
C. Cardona, A.E. Kaifer, Abstr. Pap. Am. Chem. Soc. 216 (1998) 030;
C.M. Cardona, A.E. Kaifer, J. Am. Chem. Soc. 120 (1998) 4023;
H. Tokuhisa, M.Q. Zhao, L.A. Baker, V.T. Phan, D.L. Dermody, M.E. Garcia, R.F. Peez, R.M. Crooks, T.M. Mayer, J. Am. Chem. Soc. 120 (1998) 4492;
C.F. Shu, H.M. Shen, J. Mater. Chem. 7 (1997) 47;
A. Miedaner, C.J. Curtis, R.M. Barkley, D.L. Dubois, Inorg. Chem. 33 (1994) 5482;
G.E. Oosterom, R.J. van Haaren, J.N.H. Reek, P.C.J. Kamer, P.W.N.M. van Leeuwen, Chem. Commun. (1999) 1119;
P. Jutzi, C. Batz, B. Neumann, H.-G. Stammler, Angew. Chem. Int. Ed. 35 (1996) 2118;
B. Alonso, I. Cuadrado, M. Morán, J. Losada, J. Chem. Soc. Chem. Commun. (1994) 2575;
J.-L. Fillaut, D. Astruc, J. Chem. Soc. Chem. Commun. (1993) 1320;
S. Sengupta, S.K. Sandhukhan, Organometallics 20 (2001) 1889;
S. Sengupta, S.K. Sadhukan, Tetrahedron Lett. 42 (2001) 3659;
D.L. Stone, D.K. Smith, P.T. McGrail, J. Am. Chem. Soc. 124 (2002) 856;
P.R. Ashton, V. Balzani, M. Clemente-Leon, B. Colonna, A. Credi, N. Jayaraman, F.M. Raymo, J.F. Stoddart, M. Venturi, Chem. Eur. J. 8 (2002) 673.
[50] S. Nlate, J. Ruiz, J. C. Blais, D. Astruc, Chem. Commun. (2000) 417.
[51] T.M. Miller, T.X. Neenan, R. Zayas, H.E. Bair, J. Am. Chem. Soc. 114 (1992) 1018.
[52] J. Palomero, J.A. Mata, F. Gonzalez, E. Peris, New J. Chem. 26 (2002) 291.
[53] I. Cuadrado, M. Moran, C.M. Casado, B. Alonso, F. Lobete, B. Garcia, M. Ibisate, J. Losada, Organometallics 15 (1996) 5278.
[54] J.B. Flanagan, S. Margel, A.J. Bard, F.C. Anson, J. Am. Chem. Soc. 100 (1978) 4248.